Desalination and Water Treatment
www.deswater.com

doi: 10.1080/19443994.2016.1193824

57 (2016) 28749–28754
December

Taylor & Francis
Taylor & Francis Group

Effect of shock oxidation on nitrification in raw water distribution system

Kun Xiang, Yanling Yang*, Xing Li, Da Zhang, Zhiwei Zhou, Yongwang Liu, Shuai Wang

Key Laboratory of Beijing for Water Quality Science and Water Environment Recovery Engineering, Beijing University of Technology, Beijing 100124, China, Tel. +86 10 67391726; emails: xk0807@163.com (K. Xiang), yangyanling@bjut.edu.cn (Y. Yang), lixing@vip.163.com (X. Li), 953389131@qq.com (D. Zhang), hubeizhouzhiwei@163.com (Z. Zhou), lyw2006041130@163.com (Y. Liu), 337931201@qq.com (S. Wang)

Received 9 June 2015; Accepted 19 May 2016

ABSTRACT

In this study, the nitrification performance in terms of ammonium (NH_4^+-N), nitrite (NO_2^--N), and nitrifiers activity aftershock oxidation of sodium hypochlorite (NaOCl), chlorine dioxide (ClO_2), or the combination of both (NaOCl/ClO_2) within a raw water distribution system (RWDS) was investigated. The biofilm structure was evaluated to explore its role in nitrification recovery. Our results indicate that nitrification could be recovered, although oxidation initially played an adverse role in nitrification. Compared to individual NaOCl or ClO_2, the combination of NaOCl/ClO_2 had a less negative effect on NH_4^+-N and NO_2^--N removal, as well as on the regrowth of nitrifiers. The improved biofilm regrowth and consequential faster nitrification recovery after combined oxidation was mainly ascribed to the faster reaction between NaOCl/ClO_2 and surface biofilm, resulting in decreased limitation of nutrient transfer. These results revealed the synergistic effect of NaOCl/ClO_2 on nitrification recovery, and that the biofilm structure plays a key role in nitrification recovery within RWDS.

Keywords: Raw water distribution system; Nitrification; Biofilm structure; Chlorine; Chlorine dioxide

1. Introduction

A low concentration (0.25 mg/L) of ammonium (NH_4^+-N) is sufficient to cause nitrifier growth, thus leading to nitrification [1]. In biologicalnitrification, which reduces nitrogen compounds, primarily NH_4^+-N, NH_4^+-N is sequentially oxidized into nitrite (NO_2^--N) and nitrate. In general, this process deteriorates the water quality of drinking water distribution system (DWDS) by causing difficulties in maintaining adequate disinfectant residual and controlling biofilm. A DWDS is characterized by low nutrient levels and is exposed to the continuous disinfection to limit bacteria. For comparison, the untreated water of a raw water distribution system (RWDS) is micro-polluted, with no or discontinuous oxidation. Therefore, easier biofilm regrowth and higher nitrification level is expected in the RWDS compared to in the DWDS. The concentration of NH_4^+-N decreases gradually throughout the RWDS and its removal efficiency exceeded 40% [2]. Therefore, nitrification was desirable since it could improve the water quality in the RWDS. However, nitrification in the RWDS has not raised

*Corresponding author.

sufficient attention and is poorly documented, as this function is not intended by design and has been noticed only after maintenance [3].

Limnoperna fortunei is a freshwater mytilid native to mainland China that has caused biofouling and the other local or systemwide effects in the RWDS. The shock chlorine was carried out to remove the *L. fortunei* in the RWDS. This step was cautiously implemented since nitrification is influenced by the addition of chlorine [3]. In fact, bacterial regrowth still occurred with diminished presence of disinfectant residuals [4]. Thus, the bacterial regrowth and, subsequently, nitrification recovery were inevitable in the RWDS aftershock oxidation. Nevertheless, little information is available on the response and recovery ability of nitrification aftershock oxidation within the RWDS. As was previously known, nitrification responds to biofilm regardless of whether it was in the DWDS or in the RWDS. Over 95% of the biomass was located at the inner pipe wall [5]. Extracellular polymeric substances (EPS), known as the major constituent of biofilms, have many roles including enhancing bacteria adhesion, promoting structural development, providing a protective barrier, and as adsorbing and storing nutrients for biofilm growth. Oxidants could lead to biofilm detachment, or react with the EPS and subsequently affect the nitrifiers embedded in the EPS [6]. Moreover, EPS exhibit different protection mechanisms against different oxidants, displaying higher reactivity with chlorine, but lower reactivity with monochloramine [6]. As a result, the biofilm structures may differ between oxidation approaches. Recently, the impact of NaOCl on nitrification in the RWDS model has been investigated [7], but the impacts of chlorine dioxide (ClO_2) or the combination of NaOCl and ClO_2 (NaOCl/ClO_2) on nitrification have not been studied yet. Therefore, the overall purpose of this study was to identify the treatment scheme among NaOCl, ClO_2, and NaOCl/ClO_2 that allows rapid recovery of nitrification aftershock treatment in the RWDS. We focused on the regrowth of nitrifiers after oxidation, which is related to the nitrification recovery. The EPS and visual change of biofilm structure after oxidation were investigated to explore the role of biofilm structure in the recovery of nitrification in the RWDS.

2. Materials and methods

2.1. Raw water and reagents

The simulated raw water, classified into surface water III, which targets 2.5 mg/L C (dissolved organic carbon), 1.0 mg/L N (NH_4^+-N), and 0.2 mg/L P (PO_3^-) [8], was prepared by mixing local tap water (Beijing, China) with sewage, followed by dosing with humic acid and kaoline stock solution. The main characteristics of raw water were as follows: dissolved oxygen 5.1 ± 0.2 mg/L; pH 8.1 ± 0.3; NH_4^+-N 1.05 ± 0.28 mg/L; NO_2^--N 0.05 ± 0.01 mg/L. The concentrated NaOCl (Fuchen, China) was diluted with Milli-Q water to prepare the NaOCl stock solution. Chlorine dioxide stock solution was produced according to standard methods [9].

2.2. Model RWDS

An annular reactor (AR) was used as a model RWDS, which consists of 20 removable polyethylene (PE) slides to support biofilm growth. The available surface area of each slides was 18 ± 0.5 cm^2. The AR volume was 1 L and the hydraulic retention time was 2 h. The test was carried out under room temperature (20 ± 2°C). We maintained a fixed rotational speed of 50 rpm, corresponding to a shear stress of 0.25 N/m^2 [10]. The influent was continuously pumped into the reactor. The ARs were operated for seven weeks to form a steady biofilm, with the stable removal efficiencies of NH_4^+-N and NO_2^--N at 79 and 92%, respectively. The experimental setup is displayed in Fig. 1.

One of the ARs acted as a control while the other three were oxidized with NaOCl, ClO_2, and NaOCl/ClO_2, respectively. Considering different oxidation abilities under different disinfection scenarios, we used inactivation efficiency of heterotrophic bacteria (HPC) as the dose metric in this study. Consequently, the oxidized ARs were dosed with 10 mg/L (Cl_2) NaOCl, 5 mg/L ClO_2 and 10 mg/L NaOCl/5 mg/L ClO_2, respectively, and the contact time was 120 min in all cases. Samples of aftershock oxidation were labeled as 0 (d). The subsequent operation period lasted about 21 d, which served as the recovery period.

2.3. Chemical and microbial analysis

The NH_4^+-N and NO_2^--N were measured by standard methods (Chinese SEPA, 2002). The suspended ammonia-oxidizing bacteria (AOB) and nitrite-oxidizing bacteria (NOB) populations were enumerated using the most probable number (MPN) technique. The modified Soriano and Walker liquid broth media were used for culturing AOB [11]. The NOB medium had the same composition except that it contained ammonia sulfate and phenol red, and it was supplemented with 100-mg/L sodium nitrite. The inoculated tubes were sealed with silica gel plug to prevent evaporation and incubated for four weeks at 28°C in the

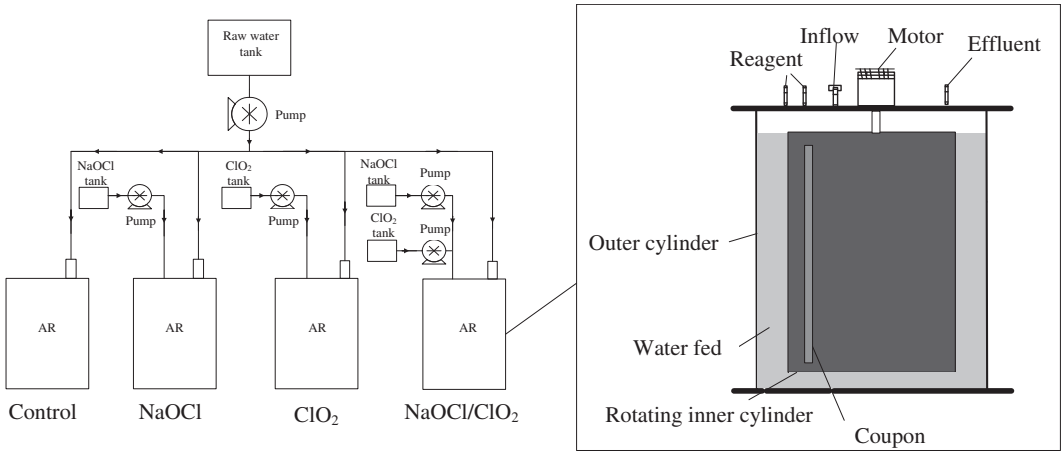

Fig. 1. Flow diagram of experiment.

dark. After incubation, the presence of AOB was determined by detecting NO_2^--N in the medium using Griess IIosvay reagent [12]. The presence of NOB was determined by detecting nitrate [11]. The PE slides covered with biofilm were removed from the ARs and transferred into a 20-ml sterile test tube containing 10-ml autoclaved phosphate-buffered saline (PBS) and 0.1% (w/v) sodium thiosulfate in tests for nitrifiers. The slides along with the saline solution were then deposited into the ultrasound for 10 min at 40 kHz. The pretreated water sample was then injected into the culture solution to be analyzed for attached nitrifiers using the same method as suspended nitrifiers.

The micrographs of the biofilms on day 0 and day 6 were measured through scanning electron microscopy (Jeol JSM 6500F, Japan) in rough vacuum conditions after the dry pretreatment [13]. Subsequently, three-dimensional surface plots of biofilm micrographs were studied using Image Pro Plus 6.0 software. The modified EDTA combined with high-speed centrifugation was employed to extract EPS. The supernatant from extraction was collected and quantified for total protein and polysaccharide. Protein was determined using the modified Bicinchoninic acid (BCA) and bovine serum albumin (BSA) as standard. Polysaccharide was measured using the anthrone-sulfuric acid method and using glucose as standard. In this study, the polysaccharide and protein were both expressed in $\mu g/cm^2$.

3. Result and discussion

3.1. Impact of shock oxidation on NH_4^+-N and NO_2^--N removal

The NH_4^+-N removal efficiencies aftershock oxidation of NaOCl, ClO_2, and NaOCl/ClO_2 are depicted in Fig. 2(a). In the control, the NH_4^+-N removal efficiency was stable around 80%, which is 30 percentage points higher than the result in a real RWDS [2]. After the addition of oxidants, the NH_4^+-N removal efficiencies abruptly decreased compared to the control, and then gradually increased until it reached a plateau at 83% on day 14. In detail, at day 0, the NH_4^+-N removal efficiencies decreased by 64, 69, and 77 percentage points for NaOCl, ClO_2, and NaOCl/ClO_2, respectively. In the following two days, the NH_4^+-N removal efficiency corresponding to NaOCl was the highest, followed by that of ClO_2 and of NaOCl/ClO_2. During days 2–14, the NH_4^+-N removal efficiency for NaOCl/ClO_2 increased most rapidly, with an improvement of 47% compared to 36% for both NaOCl and ClO_2. The result implies an interesting phenomenon in which, although the oxidation initially played an adverse role in the NH_4^+-N removal, a comparable NH_4^+-N removal efficiency as in the control after 14 d was still achieved. Furthermore, the recovery of NH_4^+-N removal for the combined oxidation was more rapid, which can be ascribed to a less negative effect of NaOCl/ClO_2 on AOB regrowth than the other two oxidants.

As seen in Fig. 2(b), the NO_2^--N removal in the control was also stable, with a mean of 92% removal during the entire experiment. The other three ARs aftershock oxidation exhibited remarkable decrease in NO_2^--N removal efficiencies, even to a minus value, especially for the initial 3 d. Unlike the continuous increase in NH_4^+-N removal efficiencies, an accumulation of NO_2^--N occurred in the initial 7 d. The accumulation of NO_2^--N probably resulted from the gradual acclimation of AOB, which implies that the oxidation of NH_4^+-N to NO_2^--N predominated in the initial recovery period. In the later phase, from day 6, the NO_2^--N removal efficiencies continuously improved.

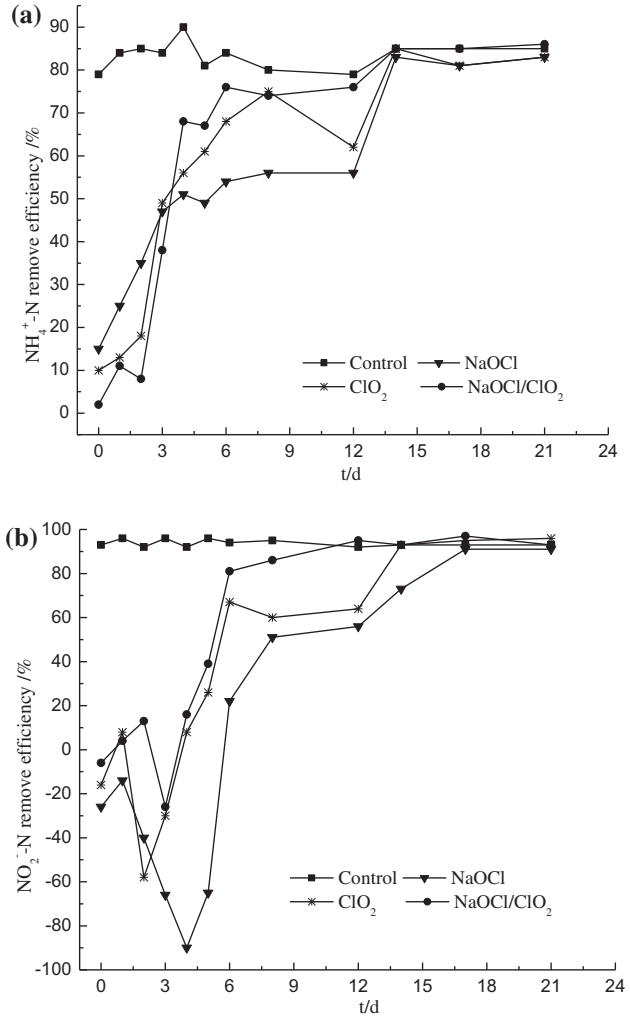

Fig. 2. Removal efficiencies of NH_4^+-N (a) and NO_2^--N (b) after NaOCl, ClO_2 and NaOCl/ClO_2.

In particular, for NaOCl/ClO_2, the removal efficiencies reached up to 95% on day 12, whereas the removal efficiencies were less than 65% for the other two oxidants, which further implies that NaOCl/ClO_2 has less negative effect on nitrification recovery.

3.2. Impact of shock oxidation on nitrifiers

The nitrifier quantities both in water (suspended) and biofilm (attached) after NaOCl, ClO_2, and NaOCl/ClO_2 are shown in Fig. 3. In general, during the entire experiment, no obvious changes of suspended nitrifiers in terms of AOB and NOB were observed in all cases, which were attributed to the detachment of attached biofilm followed by the release of nitrifiers into water. In comparison, a significant reduction in the attached nitrifiers initially occurred, and was followed by a gradual increase along the operation.

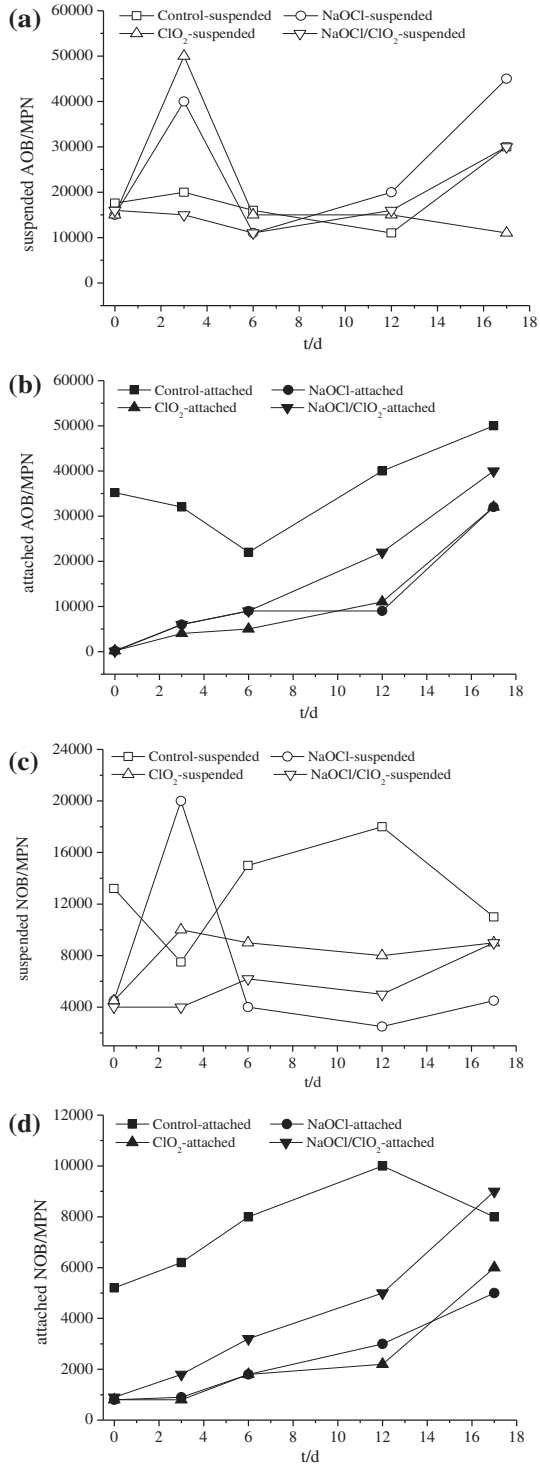

Fig. 3. AOB (a and b)/NOB (c and d) aftershock oxidation of NaOCl, ClO_2, and NaOCl/ClO_2.

As shown in Fig. 3(a), at the beginning (day 0) attached AOBs after NaOCl and ClO_2 were both 180 MPN, which was more than two times higher than that of NaOCl/ClO_2 (80 MPN). No significant difference in attached AOB among oxidant scenario was observed until day 6. On day 12, the attached AOB after NaOCl and ClO_2 were 9,000 and 11,000 MPN, respectively, which was 50% lower than that after NaOCl/ClO_2 (22,000 MPN). As shown in Fig. 3(b), the attached NOB generally showed a similar tendency as attached AOB, but with a relatively lower quantity. Again, a greater increase in attached NOB was observed after NaOCl/ClO_2 compared to the individual oxidant during the entire operation. Overall, for AOB and NOB, the regrowth rate of attached nitrifiers after NaOCl/ClO_2 was consistently faster, which well explained the previous results in Fig. 2.

3.3. Impact of shock oxidation on biofilm structure

3.3.1. Biofilm structure

Three-dimensional surface plots of biofilm after NaOCl, ClO_2, and NaOCl/ClO_2 are shown in Fig. 4. The colors of red, yellow, green, and blue correspond to the vertical distribution in biofilm. This figure shows the surface characters of biofilm and relative changes of biofilm thickness. As shown in Fig. 4(a), the distribution of biofilm formed under control conditions resembles like undulating hills, instead of a regular planar surface layer. In comparison, after NaOCl, more sparse clusters in biofilm were observed. The biofilm structures after ClO_2 or NaOCl/ClO_2 both merged into thinner structures.

After NaOCl and ClO_2, the thickness of biofilm on day 6 were smaller than those on day 0, indicating that the continuous detachment of biofilm occurred after the shock oxidation. In contrast, the biofilm structure for NaOCl/ClO_2 at day 6 was denser, although the lowest biofilm thickness was observed at the beginning. This result might mainly attribute to the improvement in nutrition transportation. The surface biofilm detachment prevailed for the chemical oxidation (chlorine) of thick biofilm, and the remaining layer was even thicker than the basal layer [14]. Therefore, the rapid regrowth after NaOCl/ClO_2 could be allowed by the faster detachment of the surface biofilm. Meanwhile, the nutrients spread more quickly into the remaining biofilm, which resulted in a faster biofilm regrowth, and subsequently the occurrence of nitrification in a relatively short period after NaOCl/ClO_2 with higher efficiency. In addition, a denser biofilm structure could enhance three-phase separation of substrates [15]. A comparison between this study and the paper by Lee et al. [15] revealed that the ammonia used by Lee et al. was about 50 times higher in concentration than that used in this study, which could be the reason why biofilm structure plays different roles in nutrient transfer.

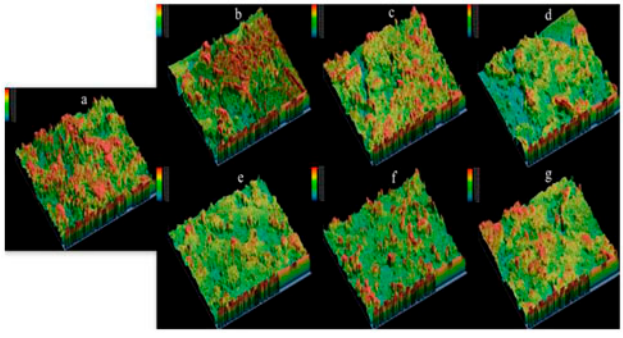

Fig. 4. Biofilm structures of control (a), NaOCl (0 day (b), 6th day (e)), ClO_2 (0 day (c), 6th day (f)) and NaOCl/ClO_2 (0 day (d), 6th day (g)).

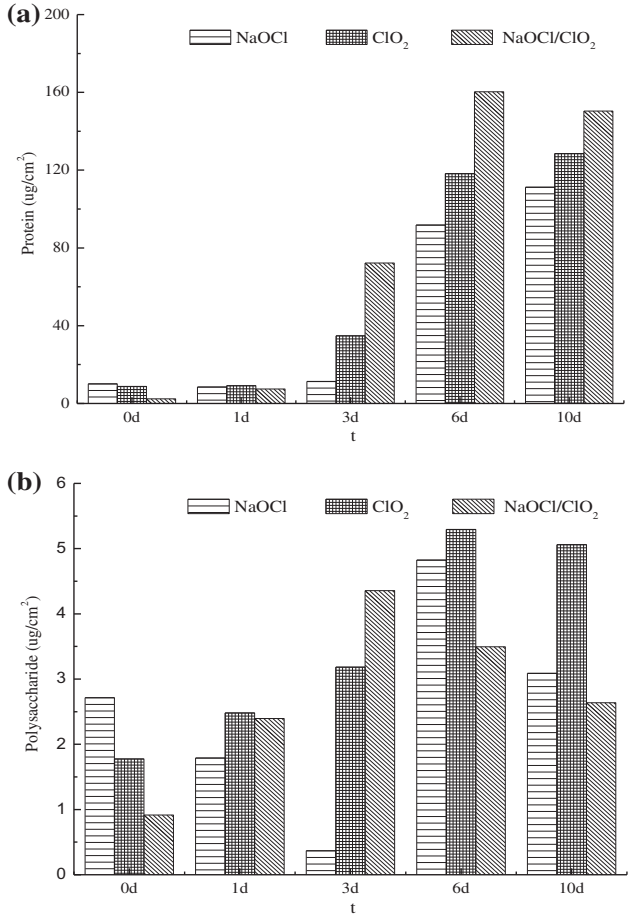

Fig. 5. Protein (a) and polysaccharide (b) after NaOCl, ClO_2, and NaOCl/ClO_2.

3.3.2. EPS content

The EPS was used to illustrate the damage and regrowth of the biofilm after oxidation. In this study, the concentrations of protein and polysaccharide in control AR were 103.5 and 9.7 $\mu g/cm^2$, respectively. This distribution of EPS contents was consistent with the previous study [16]. In comparison, a remarkable reduction in protein was observed, with less than 10 $\mu g/cm^2$ in all cases (Fig. 5(a)) during the first day. Then an increase in protein occurred after approximately 3 d of operation. In particular, in the case of $NaOCl/ClO_2$, the protein was higher than the other two oxidants, which further confirmed the result depicted in Fig. 4 that denser biofilm structure was observed after $NaOCl/ClO_2$ compared to that of the individual oxidants. Polysaccharide appeared to increase slightly during the operation, although it decreased by over 72% after oxidation (Fig. 5(b)). This different behavior, compared with protein, implies that EPS preferred to develop in proteins (enzymatic material) rather than polysaccharides (carbon 224 storage) during cell aggregation [17].

4. Conclusions

The following conclusions can be drawn from this investigation:

(1) The AR achieved a comparable nitrification level as the control after 16 d of operation, though shock oxidation initially played an adverse role in NH_4^+-N and NO_2^--N removal within RWDS.
(2) Compared to the individual NaOCl or ClO_2, $NaOCl/ClO_2$ had a less negative effect on NH_4^+-N and NO_2^--N removal, as well as on the regrowth of nitrifiers.
(3) $NaOCl/ClO_2$ exhibited the fastest destructive effect on surface structure of biofilm compared to ClO_2 or NaOCl, resulting in a decrease in the limitation of nutrient transfer, leading to better biofilm regrowth and consequential faster nitrification recovery.

Acknowledgments

This work was supported by National Natural Science Foundation of China [51178003] and Beijing Nation Science Foundation [8122013].

References

[1] M. Csanady, Nitrite formation and bacteriological deterioration of water quality in distribution system, Water Supply 10 (1992) 39–43.
[2] J. Luo, H. Liang, L. Yan, J. Ma, Y. Yang, G. Li, Microbial community structures in a closed raw water distribution system biofilm as revealed by 454-pyrosequencing analysis and the effect of microbial biofilm communities on raw water quality, Bioresour. Technol. 148 (2013) 189–195.
[3] Y. Magara, Y. Matsui, Y. Goto, A. Yuasa, Invasion of the non-indigenous nuisance mussel, *Limnoperna fortunei*, into water supply facilities in Japan, J. Water Supply: Res. Technol.-AQUA 50 (2001) 113–124.
[4] F. Codony, J. Morató, J. Mas, Role of discontinuous chlorination on microbial production by drinking water biofilms, Water Res. 39 (2005) 1896–1906.
[5] H.C. Flemming, J. Wingender, The biofilm matrix, Nat. Rev. Microbiol. 8 (2010) 623–633.
[6] Z. Xue, C.M. Hessler, W. Panmanee, D.J. Hassett, Y. Seo, *Pseudomonas aeruginosa* inactivation mechanism is affected by capsular extracellular polymeric substances reactivity with chlorine and monochloramine, FEMS Microbiol. Ecol. 83 (2013) 101–111.
[7] L. Zhao, X. Li, Y. Yang, Y. Zhu, G. Li, Destruction and restorative of nitrification performance in aqueduct by pre-chlorination, CIESE 64 (2013) 1403–1407 (in Chinese).
[8] Chinese SEPA, Environmental Quality Standards for Surface Water, Chinese Environmental Science Publishing House, Beijing, 2002.
[9] Chinese SEPA, Water and Wastewater Monitoring Methods, fourth ed., Chinese Environmental Science Publishing House, Beijing, 2002.
[10] R.R. Sharp, A.K. Camper, J.J. Crippen, O.D. Schneider, S. Leggiero, Evaluation of drinking water biostability using biofilm methods, J. Environ. Eng. 127 (2014) 403–410.
[11] N.I. Lieu, R.L. Wolfe, E.G. Means, Optimizing chloramine disinfection for the control of nitrification, J. Am. Water Works Assoc. 85 (1993) 84–90.
[12] M. Alexander, F.E. Clark, Nitrifying bacteria, in: C.A. Black (Ed.), Methods of Soil Analysis, Part 2, Chemical and Microbiological Properties, American Society of Agronomy, Madison, AL, 1965, pp. 1477–1483.
[13] M.E. Clark, R.E. Edelmann, M.L.D. Duley, J.D. Wall, M.W. Fields, Biofilm formation in *Desulfovibrio vulgaris* Hildenborough is dependent upon protein filaments, Environ. Microbiol. 9 (2007) 2844–2854.
[14] Y. Pechaud, C.E. Marcato-Romain, E. Girbal-Neuhauser, I. Queinnec, Y. Bessiere, E. Paul, Combining hydrodynamic and enzymatic treatments to improve multi-species thick biofilm removal, Chem. Eng. Sci. 80 (2012) 109–118.
[15] L.Y. Lee, S.L. Ong, W.J. Ng, Biofilm morphology and nitrification activities: Recovery of nitrifying biofilm particles covered with heterotrophic outgrowth, Bioresour. Technol. 95 (2004) 209–214.
[16] Z. Liang, W. Li, S. Yang, P. Du, Extraction and structural characteristics of extracellular polymeric substances (EPS), pellets in autotrophic nitrifying biofilm and activated sludge, Chemosphere 81 (2010) 626–632.
[17] C. Xu, S. Zhang, C.Y. Chuang, E.J. Miller, K.A. Schwehr, P.H. Santschi, Chemical composition and relative hydrophobicity of microbial exopolymeric substances (EPS) isolated by anion exchange chromatography and their actinide-binding affinities, Mar. Chem. 126 (2011) 27–36.